Nucleic Acids Research, 1997, Vol. 25, No. 12 **2455–2463**

Comprehensive, rapid and sensitive detection of sequence variants of human mitochondrial tRNA genes

Yuichi Michikawa, Götz Hofhaus+, Leonard S. Lerman[1] and Giuseppe Attardi*

Division of Biology, California Institute of Technology, Pasadena, CA 91125, USA and [1]Department of Biology, Massachusetts Institute of Technology, Cambridge, MA 02139, USA

Received January 31, 1997; Revised and Accepted April 24, 1997

ABSTRACT

In the present study, a comprehensive, rapid and sensitive method for screening sequence variation of the human mitochondrial tRNA genes has been developed. For this purpose, the denaturing gradient gel electrophoresis (DGGE) technique has been appropriately modified for simultaneous mutation analysis of a large number of samples and adapted so as to circumvent the problems caused by the anomalous electrophoretic behavior of DNA fragments encoding tRNA genes. Eighteen segments of mitochondrial DNA (mtDNA), each containing a single uniform melting domain, were selected to cover all tRNA-encoding regions using the computer program MELT94. All 18 segments were simultaneously analyzed by electrophoresis through a single broad range denaturing gradient gel under rigorously defined conditions, which prevent band broadening and other migration abnormalities from interfering with detection of sequence variants. All base substitutions tested, which include six natural mutations and 14 artificially introduced ones, have been detected successfully in the present study. Several types of evidence strongly suggest that the anomalous behavior in DGGE of tRNA gene-containing mtDNA fragments reflects their tendency to form temporary or stable alternative secondary structures under semi-denaturing conditions. The high sensitivity of the method, which can detect as low as 10% of mutant mtDNA visually, makes it valuable for the analysis of heteroplasmic mutations.

INTRODUCTION

Sequence variation of the human mitochondrial genome has lately acquired increased significance for understanding several biological processes, including evolution, diseases and aging (1–3). Our initial interest has been focused on variation of the tRNA genes, because of their central role in mitochondrial gene expression at the level of transcription, RNA processing and protein synthesis and because they appear to be the mitochondrial genes most frequently affected by mutations causing diseases in man (4–6). The rapid and sensitive method described here for screening sequence variation of the human mitochondrial tRNA genes is based on a modification (7,8) of denaturing gradient gel electrophoresis (DGGE). DGGE has been shown to be a reliable and efficient mutation screening technique (9–12). By this method, mutations are detected as producing variations in migration of the DNA fragments on denaturing gradient gels, due to the difference in denaturant concentration required for partial strand separation introduced by even a single base pair mismatch and to the fact that partially separated strands have reduced mobility when compared with their double-stranded counterpart.

In the present work the original DGGE technique has been modified for simultaneous screening of a large number of samples and adapted to correct for the unexpected anomalous electrophoretic behavior of mtDNA fragments encoding tRNA genes. In particular, a psoralen clamp has been used instead of a GC clamp to crosslink the two DNA strands (7,8), a broad range gradient of 0–80% denaturant (13) has been substituted for the commonly used narrow range gradient and a time course loading analysis has been introduced to optimize sequence variation detection in different DNA fragments. The technique described here has been tested on 20 known and artificial point mutations and every one of them has been detected.

MATERIALS AND METHODS

Cell lines

The 43B cell line carrying the $tRNA^{Leu(UUR)}$ gene A3243G mutation associated with MELAS encephalomyopathy and the 94I cell line carrying the same mtDNA without the mutation (14), the pT1 cell line carrying the $tRNA^{Lys}$ gene A8344G mutation associated with MERRF syndrome and the pT3 cell line carrying the same mtDNA without the mutation (15), the P8 cell line carrying the $tRNA^{Leu(UUR)}$ gene A3260G mutation associated with mitochondrial myopathy, cardiomyopathy, the P26 cell line carrying the same mtDNA without the mutation (16) and the lymphoblastoid cell line IV-5 carrying, immediately adjacent to the 3′-end of the $tRNA^{Ser(UCN)}$ gene, the A7445G mutation associated with non-syndromic deafness (17; M.-X.Guan,

*To whom correspondence should be addressed. Tel: +1 818 395 4930; Fax: +1 818 449 0756; Email: attardig@seqaxp.bio.caltech.edu

+Present address: Institute für Biochemie, Universität Düsseldorf, Düsseldorf, Germany

Table 1. mtDNA mutations analyzed in the present study

Type of mutation	No	Gene	Mutation[+]	Clinical[#] phenotype	Reference	MtDNA Fragment
Natural	1	$tRNA^{Leu(UUR)}$	A3243G	MELAS	31	TRNA3
	2	$tRNA^{Leu(UUR)}$	T3250C	Myopathy	18	TRNA3
	3	$tRNA^{Leu(UUR)}$	A3260G	MIMyCa	16	TRNA3
	4	$tRNA^{Ser(UCN)}$	A7445G	Deafness	17	TRNA10
	5	$tRNA^{Ser(UCN)}$	G7498A	None	19	TRNA10
	6	$tRNA^{Lys}$	A8344G	MERRF	32	TRNA13
In vitro generated	1	$tRNA^{Ile}$	A4269G	FICP	33	TRNA4
	2	$tRNA^{Ile}$	A4317G	FICP	34	TRNA4 and 5
	3	$tRNA^{Gln}$	A4340G	Not known		TRNA4 and 5
	4	$tRNA^{Met}$	T4418C	Not known		TRNA5
	5	$tRNA^{Met}$	A4469G	Not known		TRNA5
	6	$tRNA^{Trp}$	G5579A	Not known		TRNA6 and 7
	7	$tRNA^{Asn}$	A5670C	Not known		TRNA7
	8	$tRNA^{Asn}$	G5703A	PEO	4	TRNA7 and 8
	9	O_L*	G5741A	Not known		TRNA7 and 8
	10	$tRNA^{Leu(CUN)}$	A12308G	PEO	35	TRNA16
	11	$tRNA^{Leu(CUN)}$	T12311C	PEO	36	TRNA16
	12	$tRNA^{Thr}$	A15923G	LIMM	37	TRNA18
	13	$tRNA^{Thr}$	A15924G	LIMM	37	TRNA18
	14	$tRNA^{Pro}$	C15990T	Myopathy	38	TRNA18

[+]Nucleotide position (39) and change.
[#]MIMyCa, maternally inherited myopathy and cardiomyopathy; FICP, fetal infantile cardiomyopathy plus MELAS-associated cardiomyopathy; PEO, progressive external ophthalmoplegia; LIMM, lethal infantile mitochondrial myopathy.
*Region of origin of L-strand synthesis.

A.Enriquez, N.Fischel-Ghodsian and G.Attardi, unpublished data) have been previously described (see also Table 1). Similarly, reference is made to previous work for the T3250C mutation in the $tRNA^{Leu(UUR)}$ gene, which is associated with mitochondrial myopathy (18), and the presumably non-pathogenetic sequence variation at position G7498A in the $tRNA^{Ser(UCN)}$ gene (19; D.Johns, personal communication; Table 1). Two other cell lines were derived from a 20-week fetal (C1) and a 10-year-old (C2) normal individual (20).

Selection of mtDNA segments for DGGE analysis and primer synthesis

mtDNA segments containing a single uniform melting domain were selected for the DGGE analysis using the computer program MELT94 (21). Each segment is defined by the PCR primers shown in Table 2. Reducing the melting map to a single domain necessitated the choice of which end to clamp, as specified in Table 2 (22). The chosen primer oligodeoxynucleotides (Table 2) were synthesized with an Applied Biosystems 394 apparatus (ABI, Foster City, CA). One oligodeoxynucleotide of each PCR primer pair was extended at its 5′-end with a 30 bp GC clamp or linked to a psoralen clamp (7). For the latter purpose, the chosen oligodeoxynucleotides were synthesized as carrying two extra A residues and a psoralen derivative (psoralen C6 phosphoroamidite; Glen Research, Sterling, VA) at their 5′-end.

PCR amplification

Total DNA samples were prepared from unlabeled cultured cells with an Applied Biosystems 340A DNA extractor (ABI). PCR amplification of segments encoding human mitochondrial tRNA genes was performed using the Expand™ High Fidelity PCR System, following the instructions provided by the manufacturer (Boehringer Mannheim), on a DNA Thermal Cycler 480 (Perkin Elmer). The Expand™ High Fidelity PCR System consists of a mixture of Taq and Pwo DNA polymerases. Because of the inherent 3′→5′ exonuclease proofreading activity of Pwo DNA polymerase, high fidelity and specificity in PCR amplification could be obtained with this system. The $MgCl_2$ concentration in the reaction mixture was also critical for accurate amplification, an excess of $MgCl_2$ resulting in abnormal products. Accordingly, the minimum concentration of $MgCl_2$ which allowed an adequate yield of PCR product was determined for each segment and used throughout (Table 2). Temperature cycling for amplification was as follows: 94°C for 15 s, 57°C for 30 s, 72°C for 45 s; number of cycles 35.

Heteroduplex formation and photo-induced crosslinking

The aqueous phase of each PCR reaction was extracted with 100 µl chloroform and heteroduplexes between two homologous PCR products from a wild-type and corresponding mutant mtDNA were formed as described (12). Each sample to be psoralen crosslinked was placed on the cap of an Eppendorf tube 1 cm below a UV source (365 nm), consisting of 2×15 W lamps (Ultra Violet Products Inc., San Gabriel, CA) and irradiated for 15 min at 4°C. Under these conditions, 60–90% of the strands in the reannealed fragments became crosslinked, the variation in crosslinking efficiency depending upon the nature of the fragment.

Denaturing gradient gel electrophoresis

Gel apparatus and conditions were as described (11). For parallel DGGE, after annealing and crosslinking, the PCR samples were subjected to electrophoresis at 150 V in an 8% polyacrylamide gel with a linear 31.5–56.5% (narrow range) or 0–80% (broad range) denaturant gradient (100% denaturant = 7 M urea + 40% v/v formamide) parallel to the direction of electrophoresis. The appropriate running time for DGGE was determined for each DNA fragment (Table 2). The gels were stained for 10 min with ethidium bromide (1 µg/ml) and photographed with a UV transilluminator, using Polaroid type 55 black and white film.

In vitro mutagenesis

Point mutations (Table 1) were introduced into human mtDNA by the method of Ito *et al.* (23), with slight modifications. Total DNA from a mitochondrial transformant obtained by transfer of mitochondria from fibroblasts of a 20-week fetal individual into a mtDNA-less (ρ°206) cell (20) was used as the initial template for *in vitro* mutagenesis.

RESULTS

Selection of mtDNA segments

A total of 18 segments (TRNA1–TRNA18), ranging from 141 to 421 bp in length and each containing, as a result of adding the clamp, a single melting domain with a T_m of 65–74°C, were selected to cover all human mitochondrial tRNA genes using the computer program MELT94 (Table 2 and Fig. 1). Three mtDNA regions containing tRNA gene clusters (the first corresponding to $tRNA^{Ile}$, $tRNA^{Gln}$ and $tRNA^{Met}$, the second to $tRNA^{Trp}$, $tRNA^{Ala}$, $tRNA^{Asn}$, $tRNA^{Cys}$ and $tRNA^{Tyr}$ and the third to $tRNA^{Ser(UCN)}$ and $tRNA^{Asp}$), due to the difficulty of including each cluster in a fragment comprising a single melting domain, were divided into two or more partially overlapping segments (TRNA4+5, TRNA6+7+8+9 and TRNA10+11+12 respectively; Fig. 1). The overlapping portions of these segments share at least 18 nt other than their primer sequences.

Table 2. Primer sequences for DGGE analysis

No	Name	tRNA	Primer		PCR product					Running Time (h)
			Psoralen clamp	Tm (°C)	Sequence position 5'	3'	Length (bp)	Tm (°C)	$MgCl_2$ (mM)	
1	TRNA1	Phe	FOR:	60.0	523	719	197	70	1.00	3
			REV: +	60.0						
2	TRNA2	Val	FOR: +	59.8	1455	1740	286	70	1.50	3
			REV:	60.0						
3	TRNA3	Leu (UUR)	FOR:	63.1	3010	3420	411	70	0.88	5
			REV: +	65.9						
4	TRNA4	Ile and Gln	FOR:	61.6	4141	4360	220	67	0.75	2.5
			REV: +	61.8						
5	TRNA5	Ile, Gln, and Met	FOR: +	56.8	4285	4517	233	70	2.00	2.7
			REV:	57.0						
6	TRNA6	Trp	FOR: +	60.7	5460	5600	141	65	1.75	3
			REV:	55.4						
7	TRNA7	Trp, Ala and Asn	FOR: +	55.6	5544	5743	200	70	1.00	5
			REV:	61.9						
8	TRNA8	Asn and Cys	FOR: +	59.2	5658	5800	143	74	1.50	2.8
			REV:	59.2						
9	TRNA9	Cys and Tyr	FOR:	62.6	5750	6000	251	71	1.00	3
			REV: +	60.6						
10	TRNA10	Ser(UCN) and Asp	FOR:	58.5	7370	7550	181	70	2.00	3
			REV: +	57.1						
11	TRNA11	Ser(UCN) and Asp	FOR: +	59.2	7475	7700	226	65	1.00	3
			REV:	59.3						
12	TRNA12	Asp	FOR: +	55.4	7550	7680	131	69	2.00	3
			REV:	57.6						
13	TRNA13	Lys	FOR:	59.8	8237	8484	248	68	1.00	3
			REV: +	60.0						
14	TRNA14	Gly	FOR:	56.6	9950	10100	151	65	1.50	3
			REV: +	56.8						
15	TRNA15	Arg	FOR:	56.4	10350	10515	166	65	1.00	3
			REV: +	56.4						
16	TRNA16	His, Ser (AGY), and Leu (CUN)	FOR:	59.3	12080	12500	421	69	1.25	5
			REV: +	58.3						
17	TRNA17	Glu	FOR:	60.3	14550	14800	251	69	1.00	5
			REV: +	59.1						
18	TRNA18	Thr and Pro	FOR: +	56.9	15800	16080	281	67	1.00	5
			REV:	57.0						

Behavior of psoralen-clamped fragments in perpendicular and parallel DGGE

Psoralen–oligonucleotide conjugates (7,8) provide a good alternative to the commonly used GC-tailed oligonucleotides, offering the advantage of a lack of strand separation at high denaturant concentration in a broad range gradient and, therefore, increasing the flexibility of use of such a gradient (see below). Preliminary experiments aimed at comparing a GC-clamped fragment with a psoralen-clamped fragment in perpendicular DGGE (with a denaturant gradient perpendicular to the direction of electrophoresis) were carried out using the fragment TRNA3, which carries the wild-type $tRNA^{Leu(UUR)}$ gene. The two types of fragments behaved similarly, exhibiting the same single melting transition at 44.1% denaturant concentration. Furthermore, the psoralen-clamped and the GC-clamped fragment revealed the presence of a fraction of uncrosslinked psoralen-tailed molecules or, respectively, of putative improperly base paired GC-tailed molecules, as revealed by complete melting of the molecules at lower than the expected T_m (not shown). Using psoralen-tailed hybrid molecules between a TRNA3 fragment carrying the wild-type $tRNA^{Leu(UUR)}$ gene and a TRNA3 fragment carrying the $tRNA^{Leu(UUR)}$ gene with the A3243G mutation associated with MELAS encephalomyopathy, two melting transitions at 43.4% and 44.1% denaturant concentrations were observed, which correspond to the expected crosslinked homoduplexes and heteroduplexes (not shown).

For the purpose of mutation screening by DGGE (12), denaturant gradients parallel to the direction of electrophoresis (hereafter referred to as parallel gels) are routinely used. To test the behavior in a parallel DGGE gel of psoralen-clamped fragments, an experiment was carried out in which heat-denatured, annealed and UV-crosslinked wild-type TRNA3 fragment (WT) or MELAS mutation-carrying TRNA3 fragment (MT) or a mixture of wild-type and mutant fragments (WT×MT) and the same samples without UV crosslinking were run for 9 h through a parallel gel containing a narrow range (31.5–56.5% concentration) denaturant gradient (Fig. 2a). The crosslinked samples of wild-type and mutant TRNA3 fragments gave single bands with nearly identical retardation levels, while the crosslinked WT×MT sample exhibited a band with the same retardation level,

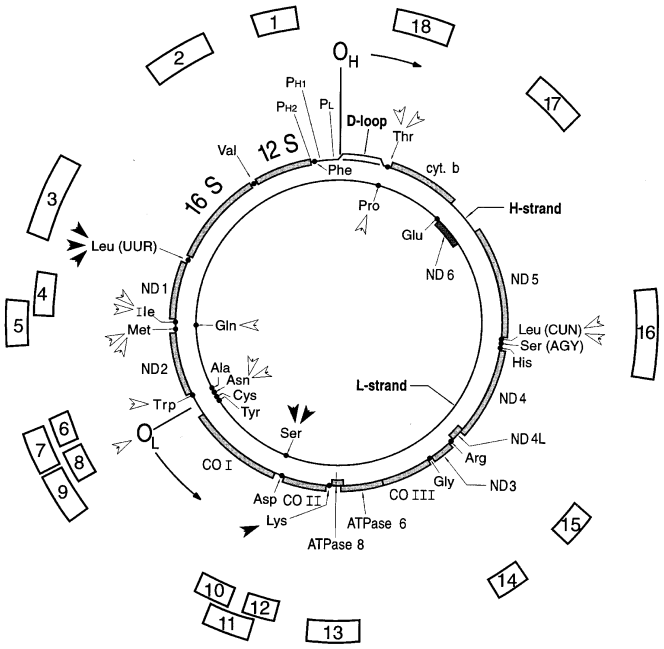

Figure 1. Map positions of human mtDNA segments amplified by PCR for sequence variation screening of tRNA genes. Eighteen segments of human mtDNA were selected to cover all tRNA-coding regions using the computer program MELT94. Natural mutations analyzed in the present study are shown by filled arrowheads, *in vitro* generated mutations by open arrowheads.

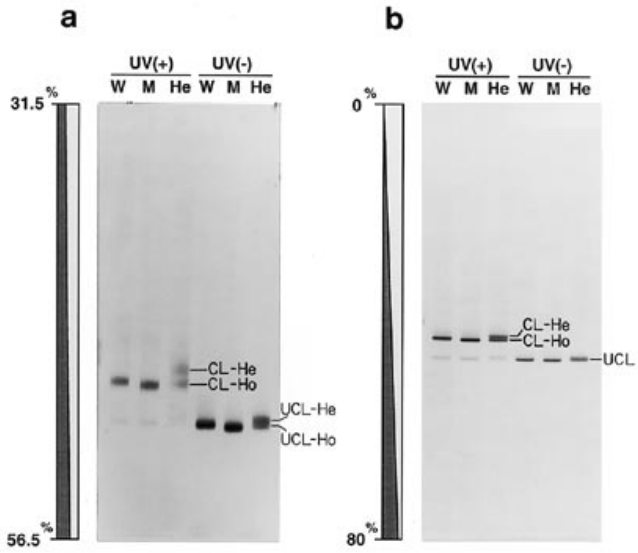

Figure 2. Parallel denaturing gradient gel electrophoresis of TRNA3. TRNA3 from wild-type cells (W) or MELAS mutation-carrying cells (M) or a mixture of TRNA3 from both cell types (He) were heat denatured, annealed, UV irradiated (UV+) or non-irradiated (UV–) and then loaded onto a narrow (31.5–56.5%) (**a**) or broad range (0–80%) (**b**) denaturant gradient gel, with the gradients being formed parallel to the direction of electrophoresis. Running time was 9 h for the narrow range and 5 h for the broad range DGGE. W, wild-type; M, mutant; CL-He, crosslinked heteroduplexes; CL-Ho, crosslinked homoduplexes; UCL, uncrosslinked molecules; UCL-He, uncrosslinked heteroduplexes; UCL-Ho, uncrosslinked homoduplexes.

consisting of homoduplex molecules (CL-Ho) and, in addition, a more retarded band of similar intensity, consisting of the two expected types of heteroduplex molecules, unresolved (CL-He). All three samples also showed a minor, faster moving band, which, by comparison with the patterns obtained with the uncrosslinked samples appeared to consist of molecules which had failed to be crosslinked during UV irradiation. Notice that uncrosslinked WT×MT exhibited a doublet of closely migrating bands (UCL-Ho and UCL-He), representing, presumably, the homoduplex and heteroduplex components.

The use of a narrow range denaturant concentration gradient was expected to limit the applicability of DGGE for simultaneous analysis of a large number of fragments carrying different mitochondrial tRNA genes, due to the fact that the various regions of interest had to be analyzed under different conditions to optimize detection of mutant mtDNA. Therefore, the broad range (0–80%) denaturant gradient (13) was tested. As shown in Figure 2b, the DGGE pattern obtained after a 5 h run in the broad range gradient showed a general similarity to that observed in the narrow range gradient after a 9 h run (Fig. 2a). However, the bands in the broad range gradient appeared to be considerably sharper and the separation between the homoduplex and heteroduplex bands was reduced.

Optimization of parallel DGGE conditions

In order to investigate the role of the steepness of the denaturing gradient and of the running time in resolution of the molecular species described in the previous section, the same heat-denatured and annealed mixture of wild-type and mutant TRNA3 fragments was used, after UV crosslinking, for a time course loading experiment on two parallel gels, one containing a narrow range (31.5–56.5%) (Fig. 3a) and the other a broad range (0–80%) (Fig. 3b) denaturant gradient. It appears that in both the narrow range gradient and, less markedly, the broad range gradient, the migration rate of the heteroduplex and homoduplex bands was reduced after a 5 h electrophoresis time. In the narrow range gradient pattern the heteroduplex and homoduplex bands were broad and not well resolved from the uncrosslinked band after a 5 or 7 h run (Fig. 3a). Furthermore, the pattern of the narrow range gradient exhibited some extra, slowly migrating bands, which could result, at least in part, from conformational changes of the TRNA3 fragment under semi-denaturing conditions (see below). In contrast, in the broad range gradient pattern the heteroduplex and homoduplex bands were sharp, clearly recognizable and well separated from the uncrosslinked band after a 5–9 h run; furthermore, there were no extra, slowly migrating bands (Fig. 3b). The above features of the DGGE pattern in a broad range denaturing gradient, the previously mentioned advantage of using a broad range gradient for simultaneous analysis of a large number of samples and the increased sensitivity of mutation detection expected from the greater apparent sharpness of the bands indicated clearly that the broad range gradient was more suitable than the narrow range gradient for mutation detection of mitochondrial tRNA genes. Accordingly, all subsequent work was carried out using this type of gradient, which allowed simultaneous analysis of up to 18 samples/gel.

The DGGE time course loading experiment of Figure 3b had insufficient resolution to determine the precise time when the uncrosslinked fragment band had passed the crosslinked fragment bands. Therefore, a higher resolution time course loading experiment was carried out. As shown in Figure 3c, the

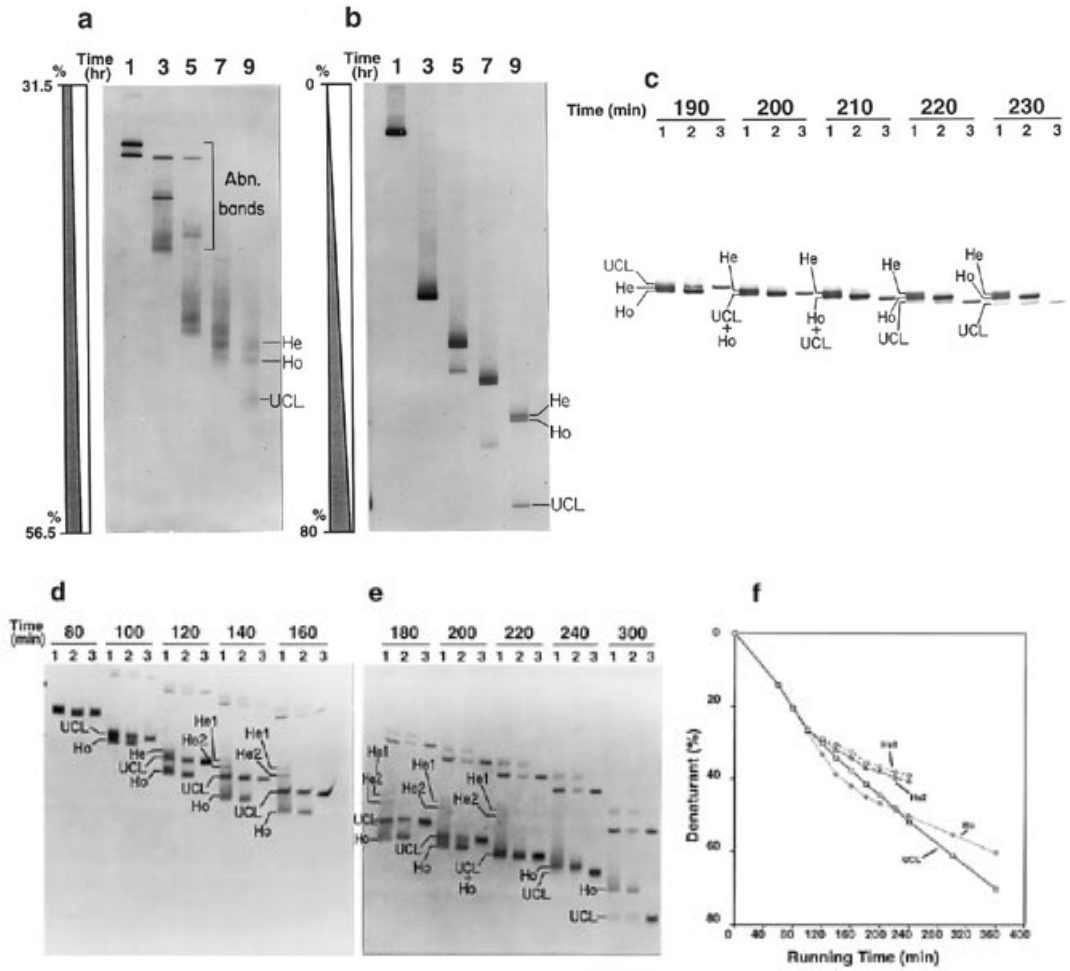

Figure 3. Detailed analysis of the migration behavior of tRNA gene-containing mtDNA fragments in a parallel denaturing gradient gel. (a, b and c) Time course loading analysis of TRNA3. A mixture of TRNA3 fragments amplified from mtDNA of wild-type and MELAS mutation-carrying cells was heat denatured, annealed, UV irradiated and then equal samples were loaded onto a narrow (**a**) or broad range (**b**) denaturant gradient gel at appropriate time intervals. (**c**) Lanes 1 show the patterns obtained when a mixture of TRNA3 fragments amplified from mtDNA of wild-type and MELAS mutation-carrying cells was heat denatured, annealed and loaded at appropriate time intervals onto a broad range denaturant gradient gel after UV irradiation, while lanes 2 and 3 show the patterns produced by wild-type TRNA3, heat denatured, annealed and loaded on the gel with or without UV irradiation respectively. (**d** and **e**) Time course loading analysis of TRNA5, which contains a cluster of three tRNA genes ($tRNA^{Ile}$, $tRNA^{Gln}$ and $tRNA^{Met}$). Lanes 1 show the products obtained when a mixture of wild-type TRNA5 and *in vitro* generated mutant TRNA5 (no. 3 in Table 1) was heat denatured, annealed and loaded at appropriate time intervals onto a broad range denaturant gradient gel after UV irradiation, while lanes 2 and 3 show the patterns produced by wild-type TRNA5, heat denatured, annealed and loaded on the gel with or without UV irradiation respectively. (**f**) The positions of migration within the denaturant gradient gel of different types of mtDNA fragments containing TRNA5 are plotted against the running time. He1 and He2, two expected heteroduplexes. Other symbols as in Figure 2.

uncrosslinked band passed the crosslinked homoduplex band after an ~220 min run, at a time when the heteroduplex and homoduplex bands were already well resolved.

It was anticipated that the presence in the different mtDNA fragment samples of a variable amount of uncrosslinked molecules could complicate recognition of the homoduplex and heteroduplex bands in a parallel DGGE pattern. Since the migration of these uncrosslinked molecules was expected to vary depending upon the T_m and the sequence of the mtDNA fragment, a time course loading analysis similar to that shown in Figure 3b for fragment TRNA3 was carried out on each of the remaining selected 17 mtDNA fragments, for the purpose of identifying the time when the uncrosslinked fragment band passed the crosslinked homoduplex band (crossover time). A time shorter than 2.5–5 h was determined for the various fragments. Since several observations had indicated that the separation between heteroduplex and homoduplex bands tended to decrease with longer electrophoresis time after the crossover time, in general a running time just longer than the estimated minimum crossover time was adopted and used as a guideline for subsequent optimization of DGGE conditions. In this way, successful recognition of the expected homoduplex and heteroduplex bands was achieved for most of the tRNA gene mutations tested (13 of 19). However, six mutations, located in two fragments (TRNA5 and TRNA8), proved to be difficult to detect, due to the absence of recognizable heteroduplex and homoduplex bands. These two fragments each contain more than one tRNA gene [$tRNA^{Ile}$, $tRNA^{Gln}$ and $tRNA^{Met}$ genes in TRNA5 and $tRNA^{Asn}$ and $tRNA^{Cys}$ genes in TRNA8, which also contains the region of origin of mtDNA light (L)-strand synthesis (O_L)], which are included in a single uniform

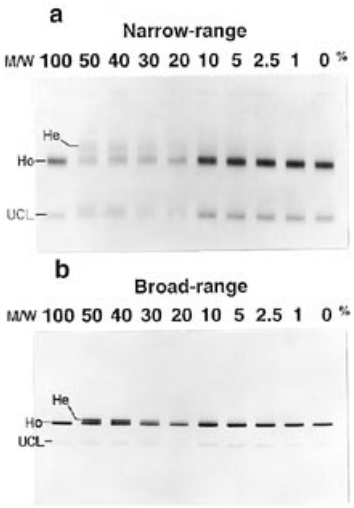

Figure 4. Analysis of sensitivity of detection of the MELAS mutation in the $tRNA^{Leu(UUR)}$ gene (TRNA3). TRNA3 fragments amplified from mtDNA of wild-type and MELAS mutation-carrying cells were quantified, combined at various ratios and used as templates for a second PCR. The products of this PCR were heat denatured, annealed and loaded onto a narrow (**a**) or broad range (**b**) denaturant gradient gel after UV irradiation. Symbols as in Figure 2.

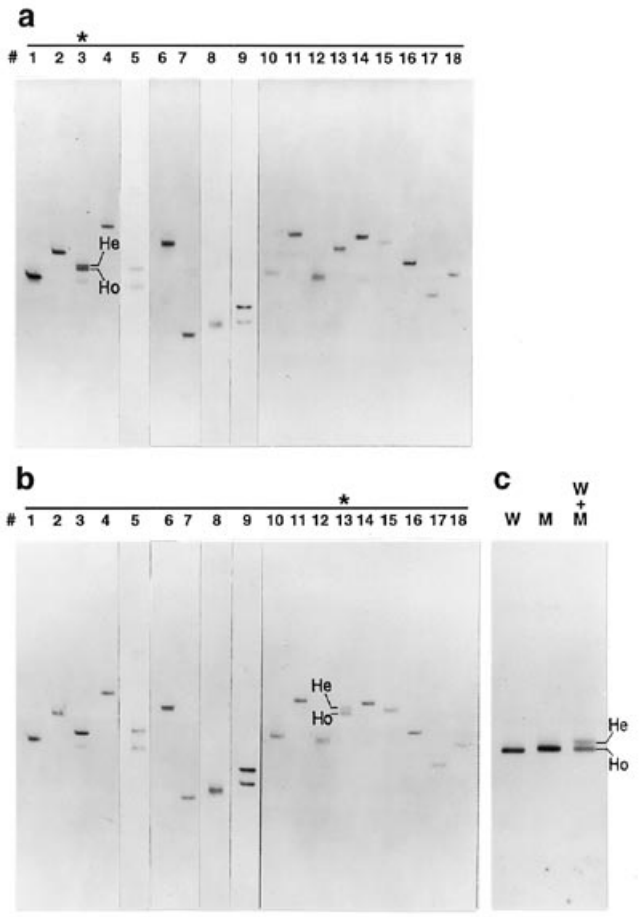

Figure 5. Simultaneous analysis in a single gel of all 18 tRNA gene-containing fragments of MELAS (**a**) or MERRF (**b**) mutation-carrying mtDNA. Annealed products formed between fragments of mtDNA from wild-type and mutant cells were loaded after UV irradiation onto a broad range denaturant gradient gel. (**c**) Confirmation of the presence of the MERRF mutation in TRNA13. W, wild-type; M, mutant. Other symbols as in Figure 2.

melting domain after addition of a GC-clamp and, presumably, also after psoralen-clamping. TRNA5 and TRNA8 behaved differently from the other fragments in parallel DGGE, in that they also produced broad bands in a broad range gradient and exhibited slowly migrating extra bands.

In order to better understand the migration properties of the components expected in a parallel DGGE run of the TRNA5 fragment carrying a tRNA gene mutation, a detailed time course loading analysis of this fragment carrying an *in vitro* generated $tRNA^{Gln}$ gene mutation (no. 3 in Table 1), of the homologous fragment carrying the wild-type gene and of hybrids thereof was carried out. As shown in Figure 3d, the two expected heteroduplex bands were separated and clearly recognizable as moving slower than the uncrosslinked fragments after a 140 min run, i.e. much before the time when the latter fragments passed the crosslinked homoduplex fragments (220–240 min); they decreased in intensity thereafter and became unrecognizable after 240 min (Fig. 3e). It should be mentioned that a comparison with the quantitative behavior of the uncrosslinked fragments and of the slowly migrating extra bands excluded a loading difference as an explanation of the apparent disappearance of the crosslinked heteroduplex fragments. The striking separation of the crosslinked heteroduplex and homoduplex bands in this DGGE run and the presence of slowly migrating extra bands should be noted. Figure 3f summarizes the behavior of the various components of TRNA5. A time course loading analysis (not shown) of the TRNA8 fragment carrying a mutation in the $tRNA^{Asn}$ gene showed a similar behavior to that of the TRNA5 fragment carrying a $tRNA^{Gln}$ mutation. Using the optimum running time determined for TRNA5 in the experiments described above, four artificially introduced tRNA gene mutations in TRNA5 could be clearly recognized by the characteristic doublet of heteroduplex bands or a single heteroduplex band more retarded than the uncrosslinked fragment band (see below). Similarly, using the optimum time determined for TRNA8, two artificial mutations (of which one was in the $tRNA^{Asn}$ gene and the other in O_L; Fig. 1) could be recognized as a single heteroduplex band more retarded than the uncrosslinked band and, respectively, as a band migrating between the uncrosslinked and crosslinked bands (see below).

Sensitivity of detection of minor proportions of mutant mtDNA

One of the advantages of the broad range denaturant gradient over the narrow range gradient is the sensitivity that it provides for mutation detection. In fact, the apparent sharpness of the bands in a broad range denaturant gradient ensures better resolution for the detection of very small proportions of mutant mtDNA. For example, the minimum proportion of mtDNA carrying the MELAS mutation which was detectable in a narrow range denaturant gradient was 20% (Fig. 4a), whereas the presence of 10% mutant mtDNA could be detected by visual inspection of the patterns in a broad range denaturant gradient (Fig. 4b).

Detection of different tRNA gene mutations

Besides the A3243G MELAS mutation discussed above, several other natural pathogenetic mutations and an innocuous polymorph-

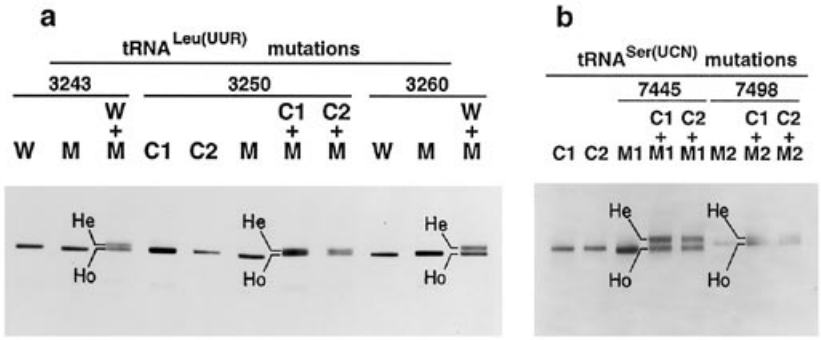

Figure 6. Detection of natural mutations in mitochondrial tRNA genes. The DGGE pattern obtained from each mtDNA fragment carrying a natural mutation in a tRNA gene was compared with that obtained from the wild-type counterpart. In cases where no wild-type counterparts of the mutation-carrying mtDNA fragments were available, the latter were compared with mtDNA fragments from two outgroup controls. The outgroup controls were mtDNA-less cell transformants carrying mtDNA from fibroblasts of a 20-week fetal individual (C1) or from fibroblasts of a 10-year-old individual (C2). Other symbols as in Figure 2.

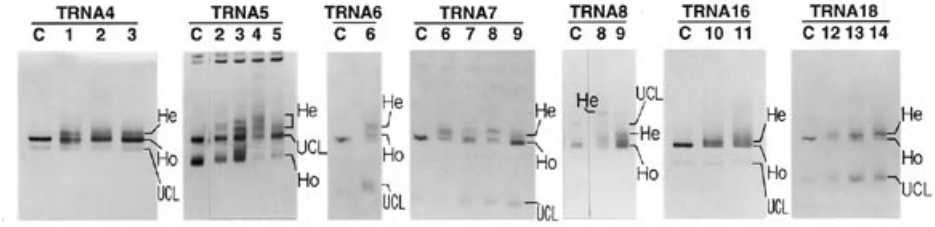

Figure 7. Detection of *in vitro* generated mitochondrial tRNA gene mutations. The point mutations listed in Table 1 were introduced*in vitro* into several mitochondrial tRNA genes of a mtDNA-less cell transformant carrying mtDNA from fibroblasts of a 20-week fetal individual as detailed in Materials and Methods. The mutated mtDNA fragments were heat denatured and annealed with the heat-denatured mtDNA fragments from the original cells and then loaded, after UV irradiation, onto a broad range denaturant gradient gel. The numbers indicate the point mutations introduced into the various mtDNA fragments, as listed in Table 1. C, wild-type mtDNA fragment. Other symbols as in Figure 2.

ism of mitochondrial tRNA genes (Table 1) were detected by the method described in the present work. In particular, the A8344G (Fig. 5) and the A3260G (Fig. 6) mutations were detected using as controls mtDNA samples from cell lines derived from the same patients but lacking the mutation. In contrast, the T3250C, T7445C and G7498A mutations were detected using as controls mtDNA samples from two transmitochondrial cell lines carrying the mtDNA from two normal young individuals (C1 and C2) (20; Fig. 6). In all cases, a doublet of heteroduplex and homoduplex bands was found in the DGGE pattern of the expected DNA fragment. In Figure 6 the DGGE runs involving mtDNAs which carried mutations at positions 3243, 3250 and 3260 in the $tRNA^{Leu(UUR)}$ gene were carried out in parallel in the same gel to test the effect of the position of the mutation on the mobility behavior of the same fragment. The striking variation in the degree of separation of the heteroduplex and homoduplex bands among the three mtDNA samples carrying different mutations in the same tRNA gene should be noted. A sequence analysis of the C1 and C2 mtDNA fragments homologous to the fragment carrying the T3250C mutation (TRNA3) or to the fragment carrying the A7445G and G7498A mutations (TRNA10) revealed that they were identical to each other and also to the homologous proband-derived specific sequence, except, in the latter case, for the variation tested for. This evidence demonstrates that the doublet of heteroduplex and homoduplex bands detected in the DGGE pattern of the expected mtDNA fragment from the proband cell lines mentioned above was due exclusively to the variation tested for. In the case of the samples utilizing the C1 and C2 normal mtDNAs as controls for the mtDNA carrying the T3250C or the G7498A mutation, four and five additional fragments and three and five additional fragments respectively exhibited retardation abnormalities in DGGE. These abnormalities presumably reflected the presence of innocuous polymorphisms.

In order to test the detectability of mutations in tRNA genes occurring in clusters in the human mitochondrial genome, many base substitutions were introduced individually into single genes in various selected mtDNA fragments from a 20-week fetal normal individual (Table 1). The corresponding PCR products were then analyzed by DGGE, in parallel with the homologous PCR products from the wild-type template. Most of these base substitutions corresponded to naturally occurring pathogenetic mutations, as specified in Table 1. As shown in Figure 7, in most cases the presence of the typical heteroduplex–homoduplex doublet was recognized in the DGGE pattern obtained from the mtDNA fragment, analyzed according to the criteria detailed in the previous sections. In the pattern of TRNA4 carrying a mutation at position 4269 in the $tRNA^{Ile}$ gene (mutation 1 in Table 1), the two individual heteroduplex bands and the two individual homoduplex bands are partially resolved. In the patterns of TRNA5 and TRNA8 there are multiple bands and their tentative identification has been discussed before. The important conclusion of these experiments is that, even in the cases of the mutant TRNA5 and TRNA8 mtDNA fragments, which have an unusual behavior in DGGE under the conditions established in the present work, one can unambiguously identify the presence of the mutation.

DISCUSSION

In the present paper an in depth analysis of the behavior in DGGE of mtDNA fragments containing tRNA genes has led to the development of a comprehensive, rapid and sensitive method for detecting sequence variation in the human mitochondrial tRNA genes. The salient features of the present method are: (i) all the 22 tRNA genes and adjacent regions of human mtDNA are included in 18 partially overlapping mtDNA segments of 141–421 bp in size, each exhibiting a single, fairly uniform melting domain as a result of adding a clamp at one end. The 18 segments together span 3126 bp of the 16 569 bp of the human mitochondrial genome; (ii) GC clamping of the original DGGE procedure has been effectively substituted by psoralen clamping, this allowing simultaneous analysis of a large number of samples over the whole broad range denaturant gradient because of the lack of strand separation in the clamp region; (iii) substitution of Taq polymerase by the Expand™ High Fidelity PCR system has dramatically increased the fidelity and specificity of PCR amplification, eliminating the need for purification of the PCR product by gel electrophoresis; (iv) use of a broad range denaturant gradient (0–80%) instead of a narrow range gradient (for example 31.5–56.5%) and rigorous definition of the optimum DGGE running time for the individual mtDNA fragments have permitted simultaneous analysis of all 18 mtDNA segments in a single gel; (v) the high sensitivity of mutation detection by the present system, which allows identification of as low a proportion of mutant mtDNA as 10% by visual inspection, permitting effective analysis of heteroplasmic mutations; (vi) identification in a total cell DNA sample of a mtDNA segment carrying a mutation and destined for subsequent sequencing analysis is very rapid, the whole procedure, from initial PCR amplification of the 18 mtDNA segments to final analysis of the ethidium bromide stained gel requiring ~36 h. Using the method described here, all 18 point mutations within mitochondrial tRNA genes, one immediately adjacent to a tRNA gene and one within O_L which were chosen for testing were detected. These mutations, which included 13 transitions known to be associated with mtDNA-linked diseases (five natural and eight generated *in vitro*), were located in different regions of the tRNA sequence.

The choice of the mtDNA to be used as a control for heteroduplex formation is an important factor in the present method. DNA from a non-affected tissue of the proband or from a proband-derived cell line not exhibiting any relevant biochemical defect (14,15) or from a non-affected tissue of a maternally related individual is suitable for this purpose. If DNA of any of the sources listed above is not available, the evidence obtained in the present work indicates that DNA from two genetically unrelated, normal individuals (preferably a fetal or young individual of the same ethnic group as the proband) can be effectively utilized to markedly reduce the number of potential fragments carrying a pathogenetic mutation, which should be further analyzed by sequencing. It should also be mentioned that the frequent occurrence of pathogenetic mtDNA mutations in heteroplasmic form (5) and the detectability of very small proportions of mutant mtDNA by the present method make it possible to directly identify a heteroplasmic mutation in a mitochondrial tRNA gene from the proband. Therefore, any abnormal DGGE pattern detected in a given mtDNA fragment during the initial screening of a mixture of putative mutant and control mtDNAs should be further investigated by a comparison of this abnormal pattern with the patterns produced separately by the putative mutant and control mtDNAs, as shown in Figures 2b and 5c.

The most intriguing result obtained in the present work has been the anomalous behavior in DGGE exhibited by the tRNA gene-containing mtDNA fragments. The most marked difference between the findings of this study and almost all previous reports on the behavior of homoduplexes and heteroduplexes in parallel DGGE has been the general appearance here of a two band pattern, rather than the typically well-resolved four band pattern. In fact, neither the homoduplex pair nor the heteroduplex pair was seen as a split band. In addition, there was a modest extent of band broadening not predicted by the calculated distribution of thermal stability in the molecule (24). Only two principal melting transitions were also observed in mixtures of mutant and wild-type fragments in perpendicular DGGE. These differences cannot be attributed to the use of the psoralen clamp instead of the GC clamp. Using an ordinary genomic sequence (the HMG box of the human *sry* gene) with the same crosslink clamp, we have observed the typical four band pattern in parallel DGGE and four principal melting transitions in perpendicular DGGE (unpublished data). Furthermore, other investigators have applied psoralen clamps routinely with normal results (7,8).

An insight into the possible factor(s) underlying anomalous migration in DGGE of the tRNA gene-containing mtDNA fragments has been provided by the observation of abnormalities in the retardation behavior of two mtDNA fragments, TRNA5 and TRNA8. The presence in TRNA5 and TRNA8 of clusters of tRNA genes called attention to the secondary structure taken by the tRNA sequences under semi-denaturing conditions as being possibly responsible for the differences in electrophoretic behavior between these fragments and the other fragments, as well as for the general absence of the typical four band pattern of homoduplexes and heteroduplexes observed with fragments containing single tRNA genes.

A detailed time course loading analysis of wild-type and mutation-carrying TRNA5 and TRNA8 revealed considerable differences in behavior in DGGE between them and the other fragments. These differences concerned the crossover time between uncrosslinked and crosslinked molecules, the denaturant concentration at which the heteroduplex molecules separated from the homoduplex molecules, the resolution of the two expected heteroduplex and homoduplex fragments and the tendency of some bands to lose resolution and disappear after long running times. The unusual behavior of the heteroduplex bands in the parallel DGGE patterns of mutation-carrying TRNA5 and TRNA8 was shown to be characteristic of the fragment rather than of the mutation. The time course analysis allowed the definition of optimum running times in DGGE for detection of mutations contained in TRNA5 and TRNA8.

Anomalous behavior of DNA fragments in DGGE has been previously described by others (24–27). In particular, attention has been called to the possible formation of temporary stem–loops, intermediate in stability between normal and fully melted forms, during DGGE (27) and to band broadening resulting from hypothetical melting intermediates, which are converted into the equilibrium melted forms at a relatively slow rate (24).

It is possible that the formation of temporary stem–loops during DGGE is responsible for the mobility abnormalities observed with TRNA5 and TRNA8. These fragments may acquire a temporary secondary structure under semi-denaturing conditions,

because they contain clusters of tRNA genes. The transient character of these secondary structures may explain the decrease in intensity of the bands and, in some cases, their apparent disappearance observed during the DGGE run of these fragments (Fig. 3d and e). Furthermore, some of the secondary structures acquired by these tRNA gene cluster-containing mtDNA fragments may be stable, as exemplified by the slowly migrating abnormal bands (Fig. 3d and e). TRNA8 also contains O_L, which is known to have a high degree of secondary structure (28). An anomalous electrophoretic behavior in denaturing polyacrylamide gels has been previously demonstrated for the excised leader of human cytochrome *c* oxidase subunit I mRNA, which contains O_L as well as the surrounding sequences of the four L-strand-encoded tRNA genes and has been attributed to an unusually stable secondary structure (29). Recently, the striking effect of the tertiary and secondary structure of mitochondrial tRNAs on their mobility in perpendicular DGGE and on separation of the aminoacylated and non-acylated forms has been reported (30).

As concerns the absence of the typical four band pattern of homoduplexes and heteroduplexes observed in the mtDNA fragments containing single tRNA genes, it appears that base substitutions and single base mismatches affected the stability versus denaturation of these fragments less than generally observed in nuclear genomic sequences previously analyzed by DGGE. This phenomenon may also be related to alternative secondary structures caused by base mismatches in the tRNA sequences, if one assumes that these conformational changes have a dominant retardation effect. In conclusion, the evidence discussed above strongly suggests that not only the primary sequence, but also transient and, in some cases, stable alternative secondary structures under semi-denaturing conditions play an important role in determining the migration in DGGE of mtDNA fragments containing tRNA genes.

ACKNOWLEDGEMENTS

These investigations were supported by NIH grant GM11726 and NIA grant AG12117-05 (to G.A.), NIH grant HG00345 (to L.L.) and by a Gosney Fellowship (to Y.M.). We are very grateful to Donald Johns, Ikuya Nonaka, Massimo Zeviani and Nathans Fischel-Ghodsian for making tissue samples and cell lines available to us and to David Page and Laura Brown for the samples of the wild-type and mutant human *sry* gene (HMG box DNA). We also thank Anne Chomyn and Antonio Enriquez for valuable discussions and Arger Drew, Benneta Keeley, Catherine Lin and Rosario Zedan for their expert technical assistance.

REFERENCES

1 Luft,R (1994) *Proc. Natl. Acad. Sci. USA*, **91**, 8731–8738.
2 Wallace,D.C. (1994) *Proc. Natl. Acad. Sci. USA*, **91**, 8739–8746.
3 Attardi,G., Yoneda,M. and Chomyn,A. (1995) *Biochim. Biophys. Acta*, **1271**, 241–248.
4 Moraes,C.T., Ciacci,F., Bonilla,E., Jansen,C., Hirano,M., Rao,N., Lovelace,R.E., Rowland,L.P., Schon,E.A. and DiMauro,S. (1993) *J. Clin. Invest.*, **92**, 2906–2915.
5 Wallace,D.C. (1992) *Annu. Rev. Biochem.*, **61**, 1175–1212.
6 Kadenbach,B., Munscher,C., Frank,V. Mullerhocker,J. and Napiwotzki,J. (1995) *Mutat. Res.*, **338**, 161–172.
7 Costes,B., Girodon,E., Ghanem,N., Chassignol,M., Thuong,N.T., Dupret,D. and Goossens,M. (1993) *Hum. Mol. Genet.*, **2**, 393–397.
8 Fernandez,E., Bienvenu,T., Arramond,F.D., Beldjord,K., Kaplan,J.C. and Beldjord,C. (1993) *PCR Methods Applicat.*, **3**, 122–124.
9 Lerman,L.S., Fischer,S.G., Hurley,I., Silverstein,K. and Lumelsky,N. (1984) *Annu. Rev. Biophys. Bioeng.*, **13**, 399–423.
10 Lerman,L.S. and Silverstein,K. (1987) *Methods Enzymol.*, **155**, 482–501.
11 Myers,R.M., Maniatis,T. and Lerman,L.S. (1987) *Methods Enzymol.*, **155**, 501–527.
12 Abrams,E.S. and Stanton,V.P. (1992) *Methods Enzymol.*, **212**, 71–104.
13 Guldberg,P. and Güttler,F. (1994) *Nucleic Acids Res.*, **22**, 880–881.
14 Chomyn,A., Martinuzzi,A., Yoneda,M., Daga,A., Hurko,O., Johns,D., Lai,S.T., Nonaka,I., Angelini,C. and Attardi,G. (1992) *Proc. Natl. Acad. Sci. USA*, **89**, 4221–4225.
15 Chomyn,A., Meola,G., Bresolin,N., Lai,S.T., Scarlato,G. and Attardi,G. (1991) *Mol. Cell. Biol.*, **11**, 2236–2244.
16 Mariotti,C., Tiranti,V., Carrara,F., Dallapiccola,B., Didonato,S. and Zeviani,M. (1994) *J. Clin. Invest.*, **93**, 1102–1107.
17 Prezant,T.R., Shohat,M., Jaber,L., Pressman,S. and Fischel-Ghodsian,N. (1992) *Am. J. Med. Genet.*, **44**, 465–472.
18 Goto,Y., Tojo,M., Tohyama,J., Horai,S. and Nonaka,I. (1992) *Ann. Neurol.*, **31**, 672–675.
19 Johns,D.R., Hurko,O., Attardi,G. and Griffin,J.W. (1991) *Ann. Neurol.*, **30**, 234.
20 Laderman,K.A., Penny,J.R., Mazzucchelli,F., Bresolin,N., Scarlato,G. and Attardi,G. (1996) *J. Biol. Chem.*, **271**, 15891–15897.
21 Lerman,L.S., Silverstein,K., Fripp,B., Sauer,P. and Dresselhaus,C. (1996) http://web.mit.edu/osp/www/melt.html.
22 Myers,R.M., Fischer,S.G., Maniatis,T. and Lerman,L.S. (1985) *Nucleic Acids Res.*, **13**, 3111–3129.
23 Ito,W., Ishiguro,H. and Kurosawa,Y. (1991) *Gene*, **102**, 67–70.
24 Abrams,E.S., Murdaugh,S.E. and Lerman,L.S. (1995) *Nucleic Acids Res.*, **23**, 2775–2783.
25 McCampbell,C.R., Wartell,R.M. and Plaskon,R.R. (1989) *Biopolymers*, **28**, 1745–1758.
26 Gray,M., Charpentier,A., Walsh,K., Wu,P. and Bender,W. (1991) *Genetics*, **127**, 139–149.
27 Weber,C.K., Shaffer,D.J. and Sidman,C.L. (1991) *Nucleic Acids Res.*, **19**, 3331–3335.
28 Wong,T.W. and Clayton,D.A. (1985) *Cell*, **42**, 951–958.
29 Gaines,G., Rossi,C. and Attardi,G. (1987) *Mol. Cell. Biol.*, **7**, 925–931.
30 Enriquez,J.A. and Attardi,G. (1996) *Proc. Natl. Acad. Sci. USA*, **93**, 8300–8305.
31 Goto,Y., Nonaka,I. and Horai,S. (1990) *Nature*, **348**, 651–653.
32 Shoffner,J.M., Lott,M.T., Lezza,A.M.S., Seibel,P., Ballinger,S.W. and Wallace,D.C. (1990) *Cell*, **61**, 931–937.
33 Hayashi,J.I., Ohta,S., Kagawa,Y., Takai,D., Miyabayashi,S. and Tada,K. (1994) *J. Biol. Chem.*, **269**, 19060–19066.
34 Ito,T., Hattori,K., Obayashi,T., Tanaka,M., Sugiyama,S. and Ozawa,T. (1992) *Jap. Circulat. J.*, **56**, 1045–1053.
35 Houshmand,M., Larsson,N.G., Holme,E., Oldfors,A., Tulinius,M.H. and Andersen,O. (1994) *Biochim. Biophys. Acta*, **1226**, 49–55.
36 Hattori,Y., Goto,Y., Sakuta,R., Nonaka,I., Mizuna,Y. and Horai,S. (1994) *J. Neurol. Sci.*, **125**, 50–55.
37 Yoon,K.L., Aprille,J.R. and Ernst,S.G. (1991) *Biochem. Biophys. Res. Commun.*, **176**, 1112–1115.
38 Ionasescu,V.V., Hart,M., DiMauro,S. and Moraes,C.T. (1994) *Neurology*, **44**, 975–977.
39 Anderson,S., Bankier,A.T., Barrell,B.G., de Bruijin,M.H.L., Coulson,A.R., Drouin,J., Eperon,I.C., Nierlich,D.P., Roe,B.A., Sanger,F., Schreier,P.H., Smith,A.J.H., Staden,R. and Young,I.G. (1981) *Nature*, **290**, 457–465.